International Journal of Advanced Multidisciplinary Research

ISSN: 2393-8870 www.ijarm.com

(A Peer Reviewed, Referred, Indexed and Open Access Journal)
DOI: 10.22192/ijamr Volume 12, Issue 11-2025

DOI: http://dx.doi.org/10.22192/ijamr.2025.12.11.002

Research Article

Phytogenic Silver Nanoparticles: Green Synthesis for their Dual Bioactivity against Microbes and Malaria Parasites

M.C. Gangorde¹ and Vatsal M. Patel²

1- Department of Chemistry, Government Science College, Songadh, Gujarat, India.

2- J.N.M. Patel Science College, Barthana, Vesu, Surat.

Affiliated with: Veer Narmad South Gujarat University, Surat, Gujarat, India

*Corresponding Author: manishgangorde@gmail.com/

Manishkumar.Gangorde@gujgov.edu.in

Abstract

Keywords

Silver Nanoparticles (AgNPs),
Green Synthesis,
Chloris virgata,
Anti-microbial activity,
Anti-plasmodialactivity,
Phytogenic synthesis,

Chloris virgata, a resilient grass of the Poaceae family, is widely distributed in warm climates and traditionally used for wound healing and livestock fodder. Its unique phytochemical composition and stress-tolerant nature have recently drawn interest for nanobiotechnology. In the present study, an aqueous extract of *C. virgata* was employed for the green synthesis of silver nanoparticles (AgNPs). Reduction of Ag⁺ ions from silver nitrate was achieved using thermal and microwave treatment, evidenced by a colour change from light red to dark brown. Characterization through UV–Vis, FTIR, XRD, SEM, and HR-TEM confirmed the formation of crystalline, predominantly spherical AgNPs with sizes ranging from 5.7 to 52.5 nm. The nanoparticles exhibited antimicrobial activity against Gram-positive and Gramnegative bacteria, fungi, and Plasmodium falciparum, producing inhibition zones of 8–28 mm with MIC values of 62.5–1000 μg/mL. Though less potent than standard drugs, their broad-spectrum efficacy highlights *C. virgata* 's promise as a sustainable source for nanomedicine.

Introduction

Chloris virgata is a grass species appreciated by livestock; it provides good fodder, but is not productive. Medicinal: Crushed leaves of Chloris virgata, which are then soaked in water, are applied to wounds to prevent infection. Chloris virgata belonging to the Poaceae family, is a weed of warm weather in the eastern part of Australia, and its occurrence can be easily observed throughout the mainland of Australia. Resistance or tolerance to glyphosate, dispersal through flooding and wind, and greater production of seeds are factors that result in the prevalence of Chloris virgata in both noncropping and cropping seasons (Mahajan G et al. 2021, Rojas-Sandoval 2022). Different transcriptomic analyses were performed on Chloris virgata, which reported the major genes responsible for its fastest growth and germination, especially in the major grasslands of Mongolia (Bolortuya B 2021). Chloris virgata is an alkaliresistant halophyte that thrives under conditions of high buffer capacity and pH (pH 9.6). Therapeutically, it has shown an equal zone of inhibition against Escherichia coli, Salmonella Proteus mirabilis. and Klebsiella tvphi. pneumonia due to the availability of different phyto compounds. After soaking in water, the crushed leaves of Chloris virgata can be applied to wounds to prevent infection. According to the literature survey, details about the authentication, use of this plant as a source of phyto compounds, or antioxidant activity are available. (Dolly Kumari et al. 2024)

Nanoparticles are defined as particles with at least one dimension ranging from 1 to 100 nanometers. Owing to their extremely small size, nanoparticles exhibit unique physical, chemical, and biological properties that differ significantly from those of their bulk counterparts (Kumar et al., 2019; Bhushan, 2017). These distinct characteristics primarily arise from the increased surface-area-to-

volume ratio and quantum effects, which become prominent at the nanoscale.

The enhanced surface area of nanoparticles, sometimes up to 35-45% greater than that of larger particles, enables superior reactivity and interaction with biological and chemical environments (Saqib et al., 2022; Azam et al., 2020). This attribute is particularly beneficial in various scientific fields, such as molecular biology, organic inorganic physics, and chemistry, medicine, and materials science. Owing to these advantageous properties, nanoparticles have been extensively applied in areas such as drug delivery, imaging, catalysis, environmental remediation, and electronic device fabrication (Vu et al., 2021; Rajapaksha et al., 2023; Doan et al., 2023). Recent developments in nanotechnology have focused not only on producing nanoparticles with precise sizes and shapes, but also on employing environmentally sustainable, cost-effective, and scalable synthesis methods that can be customized for specific end uses.

Silver nanoparticles (AgNPs) are highly versatile nanomaterials with unique physical, chemical, and biological properties. Their well-documented anti-microbial activity makes them widely used in medicine, textiles, water purification, and wound healing applications. (Lu, 2016; M.C. Gangorde, 2024) Beyond anti-bacterial uses, AgNPs play key roles in drug delivery, cancer therapy, biosensing, and diagnostics, offering benefits like improved drug stability, targeted delivery, and controlled release. Their optical and electrical properties also support applications in electronics, such as conductive inks and sensors, as well as in consumer products, such as cosmetics and food packaging. (Emelda Orlando Simbine et al., 2019; Nemčeková K et al., 2025; Y.Z.N. Htwe, 2022; Gomeceria, 2024; Gajbhiye et al., 2016) Among various metallic nanoparticles, nanoparticles (AgNPs) have garnered significant attention due to their exceptional anti-microbial, optical, and catalytic properties. Multiple

synthetic routes have been established for the production of AgNPs, broadly categorized into chemical, physical, photochemical, and biological (or green synthesis) methods (Barabadi et al. 2017b; Yaqoob et al., 2020).

In this research, we have represented the green synthesis of silver nanoparticles by reducing the silver ions present in the solution of silver nitrate (AgNO₃) by an aqueous rootless plant extract of Chloris Virgata. Silver nanoparticles (AgNPs) were successfully designed and generated by treating AgNO₃ solution at 70°C for 30 min. and then placed in a microwave for 5 min at 2450 MHz power levels ranging from 350 W to 850 W. The colour change of the plant extract of Chloris virgata treated solution from light brown to dark brown confirmed the formation of silver nanoparticles, and the nature of the synthesized nanoparticles was characterized by UV-Vis spectroscopy, FT-IR(Fourier Transform Infrared spectroscopy), X-ray diffraction, SEM(Scanning

Electron Microscopy), and HR-TEM(High Resolution Transmission Electron Microscopy). AgNPs exhibit excellent anti-bacterial properties. This study provides a significant basis for applying AgNPs as antimetabolites and medicated AgNPs to play a major role in the field of nanomedicine.

Materials and Methods

Collection of the material

Chloris virgata is widely found in the Dang and Tapi districts. Plant samples were collected from the campus of the Government Science College, Songadh, Tapi district. (Lat-21.12 and Long. 73.40.) the whole plant was used without roots, and the plant was washed, shade-dried, and powdered in a kitchen grinder. Silver nitrate was purchased from Sigma–Aldrich. Here fig.1 indicates Chloris virgata plant.



Fig. 1 Chloris virgata plant

Method

Preparation of aqueous plant extract.

Fresh whole plants without roots were collected and washed with double distilled water, shadedried, and pulverized using a kitchen grinder. Powdered plants (Shawn in fig.2) were stored in airtight containers for future use in the green synthesis of the silver nanoparticles. Plant powder (15 g) was added to double-distilled water and shaken thoroughly. The prepared mixture was refluxed for 2 h 30 min at 60°C(Shawn in fig.3) and the hot mixture was filtered through Whatman filter paper no. 1. The aqueous extract (Shawn in fig.4) was refrigerated at 4°C and used as a stock solution for AgNPs synthesis.



Fig.2 Powder form of *Chloris virgata* plant

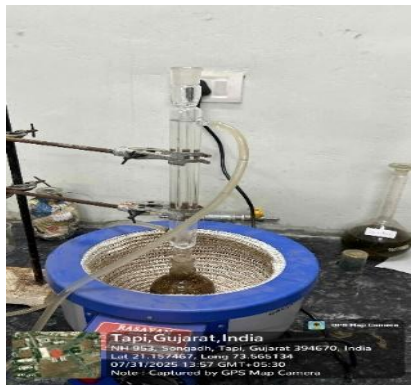


Fig.3 Extract reaction apparatus



Fig.4 Plant extract

Synthesis of AgNPs using of aqueous plant extracts

For the bio-mediated synthesis of silver nanoparticles, 40 ml of 1 mM AgNO₃ salt solution was slowly added to 25 ml of the plant extracts. After completion of the addition, the reaction mixture was kept on a magnetic stirrer with a hot plate for 30 min. at 70°C and then placed in a microwave for 5 minutes at 2450 MHz power levels ranging from 350 W to 850 W. The colour change was observed between reaction solutions after adding AgNO₃. The colour change indicated that AgNPs were generated. Here, the colour changed from red to dark brown. The reduction of Ag+1 to Ag0 was mediated by the biomolecules present in the plant, which acted as reducing and capping agents. (Kabeya et al., 2025; Do et al., 2025; Liknaw et al., 2025; Abd El Aty et al., 2025; Plesnicute et al., 2025; Singh et al., 2025) and in vitro anti-plasmodial activity. (Kojom Foko et al., 2025; Nafa et al., 2025)

Further confirmation of AgNPs was performed using UV–Vis spectral analysis with absorbance peaks from 420 to 460 nm. After this confirmation, the reaction mixture was subjected to centrifugation to isolate the silver nanoparticles at 10000 rpm for 30 min to isolate the AgNPs. The separated nanoparticles settled at the bottom, were collected, washed with double-distilled water, and then dried in a hot air oven at 60°C for 1 h 30 min. Finally, the powdered AgNPs were stored at 4°C for further characterization and identification of an anti-microbial zone of inhibition.

Anti-microbial activity

Accurate evaluation of anti-microbial efficacy is essential for pharmaceutical development and clinical microbiology. The choice of method for anti-microbial testing depends on the objective of the study and nature of the test compound. (Hamid LL et al. 2024; CLSI, 2020; R.M. Varghese et al., 2024; S K Sahu et al. 2025)

Zone of Inhibition (ZOI) for Anti-bacterial and Anti-fungal Activity

The Agar Cup Diffusion Method was employed to assess the anti-microbial efficacy of the synthesized compounds. (CLSI 2023; De Mel S, et al. 2025; Ahmad N, et al. 2024; Singh RK, et al. 2025) This is a standardized, non-automated in vitro method widely used to evaluate the susceptibility of microorganisms to anti-microbial agents by measuring the zone of inhibition (ZOI) (in mm), which corresponds to the area around the well where microbial growth is inhibited. (Iwuji C, et al. 2024; Keerthiga G, et al. 2025) The standard microbial strains for gram positive bacteria as Staphylococcus aureus (MTCC 86) and Streptococcus pyogenes (MTCC 443) for Gram-negative Escherichia coli (MTCC 442) and Pseudomonas aeruginosa (MTCC 441) were used for evaluating anti-bacterial and for Anti-fungal activity Candida albicans (MTCC Aspergillus niger (MTCC 282) and Aspergillus clavatus(MTCC 1323) were used as test organisms. All strains were procured from the Microbial Type Culture Collection (MTCC) at Institute of Microbial the Technology, Chandigarh.

In Vitro Antimalarial Screening

All the synthesized compounds were screened for antimalarial activity in the Microcare Laboratory & TRC, Surat, and Gujarat.

The in vitro antimalarial assay was carried out in 86-well microtiter plates according to the microassay protocol of Rieckmann et al. with minor modifications. The cultures of P. falciparum 3D7 were maintained in medium RPMI 1640 supplemented with 25 mM HEPES, 1% D-glucose, 0.23% sodium bicarbonate, and 10% heat-inactivated human serum. (Srinivasa SB et al. 2025; Bestgen B et al. 2025) for observations of the in vitro antimalarial screening of the mean number of rings, trophozoites, and schizonts recorded per 100 parasites from duplicate wells after incubation for 38 h and percent maturation inhibition with respect to the control group.

Results and Discussion

The formation of AgNPs was indicated by a colour change of the solution from light red to dark brown. (Fig.5)

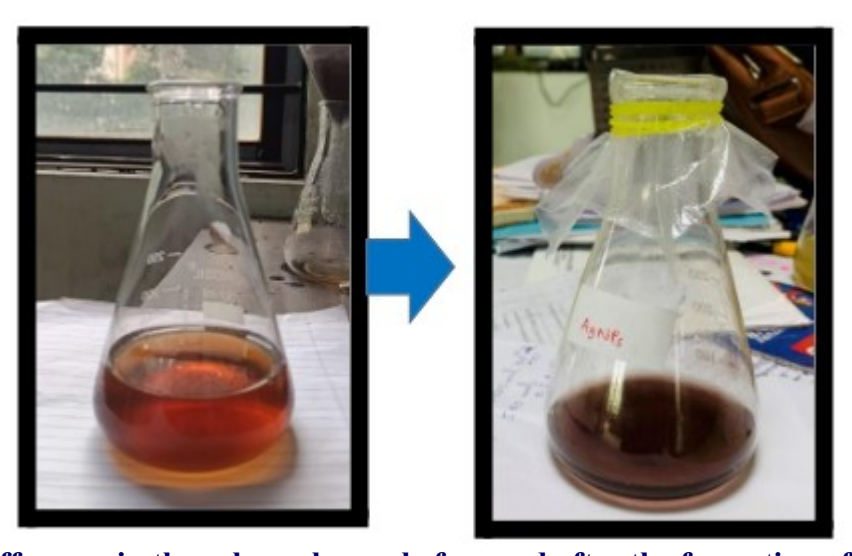


Fig. 5 Difference in the colour change before and after the formation of AgNPs.

UV-Visible Spectroscopy

UV-Visible Spectroscopy analysis was performed using a Varian Cary 50 UV-Vis spectrophotometer. The absorption spectra of the synthesized silver nanoparticles were recorded in distilled water. Fig. 6a shows the UV-visible spectra of AgNO₃ soln., which has an absorption peak at 214 nm. Fig. 6b shows the UV-visible spectra of the plant extracts with an absorption peak at 375 nm. Fig. 6c shows the UV-visible

spectra of silver nanoparticle formation and the colour change of the solution from dark red to dark brown, depending on the concentration of the extract and inclusion of the silver nitrate solution. With time, the concentration of AgNPs increased, and the peak value increased accordingly and became sharper from 420 nm to 465 nm. These results are similar to those of other researchers (Sana et al. 2018; Maarebia et al. 2018; Bali et al. 2025)

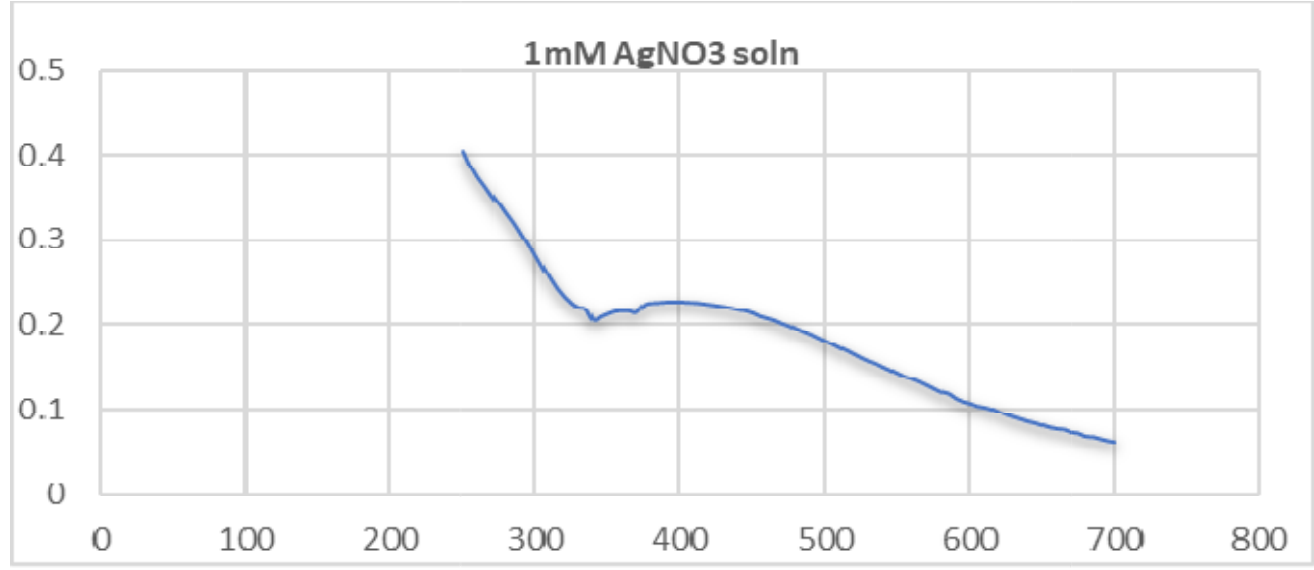


Fig. 6a shows the UV-Visible spectra of AgNO₃ soln.

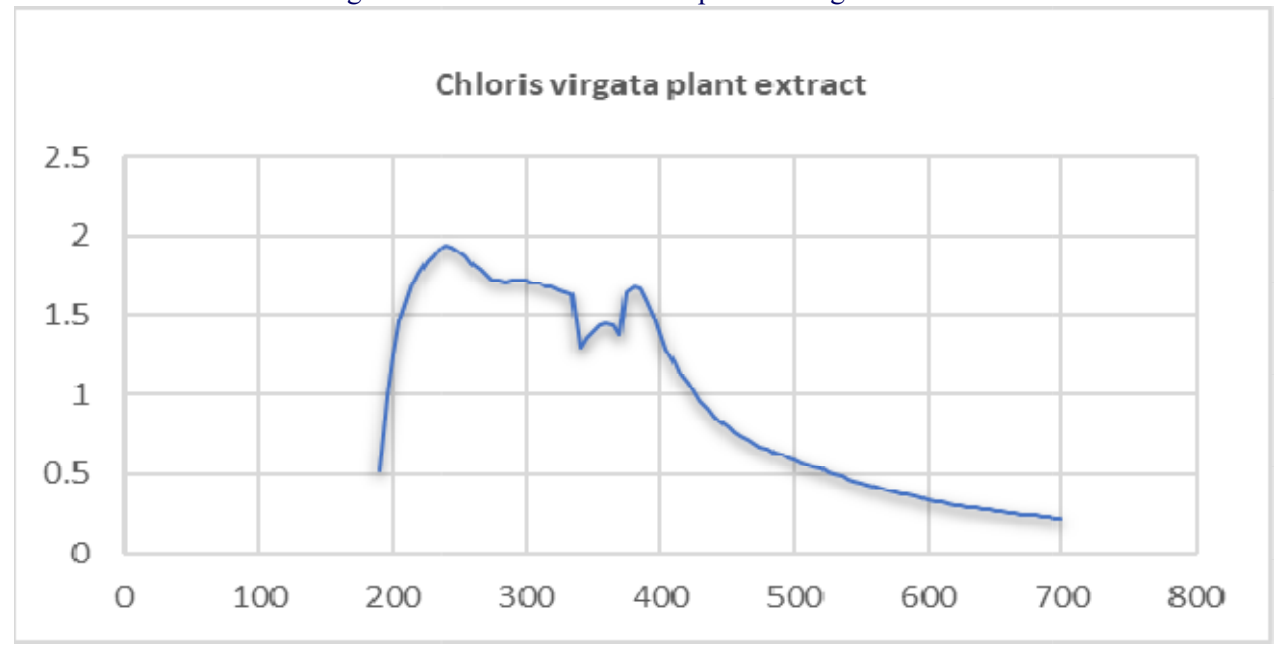


Fig. 6b shows the UV- Visible spectra of plant extracts

Int. J. Adv. Multidiscip. Res. (2025). 12(11): 17-34

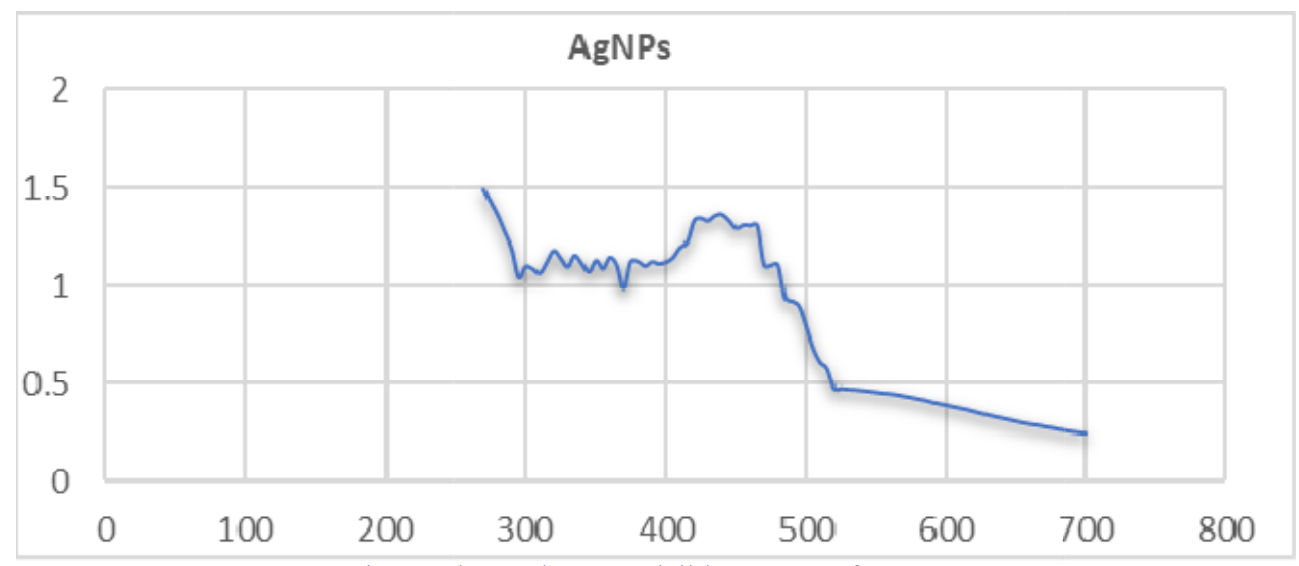


Fig. 6c shows the UV Visible spectra of AgNPs

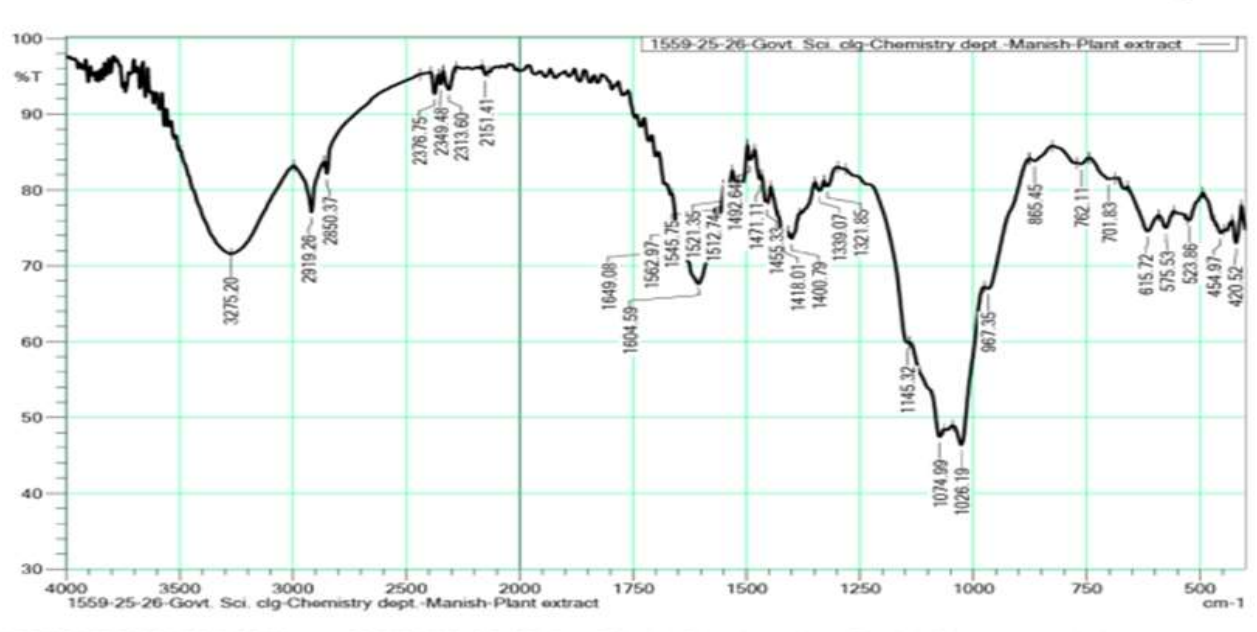
Fourier Transform Infrared spectroscopy (FTIR)

FTIR Analysis for AgNPs

FT-IR analysis was performed using a Bruker, Germany, Model 3000 Hyperion Microscope with a Vertex 80 FTIR System, ranging from 80 cm⁻¹ to 25000 cm⁻¹. Approximately 0.1 ml, or a single drop, of AgNPs was used for preparing liquid

samples in FTIR. The most common method involves sandwiching a thin layer of the liquid between two salt plates (like NaCl or KBr) and subjecting it to FT-IR spectroscopy measurement range set from 400 cm⁻¹ to 4000 cm⁻¹. Fig. 7a and 7b show the FT-IR spectra. As like Silver nanoparticles FTIR reference research papers (Riaz et al., 2018; Mamand et al., 2025; Pasieczna-Patkowska et al., 2025).

SICARI, V.V. Nagar

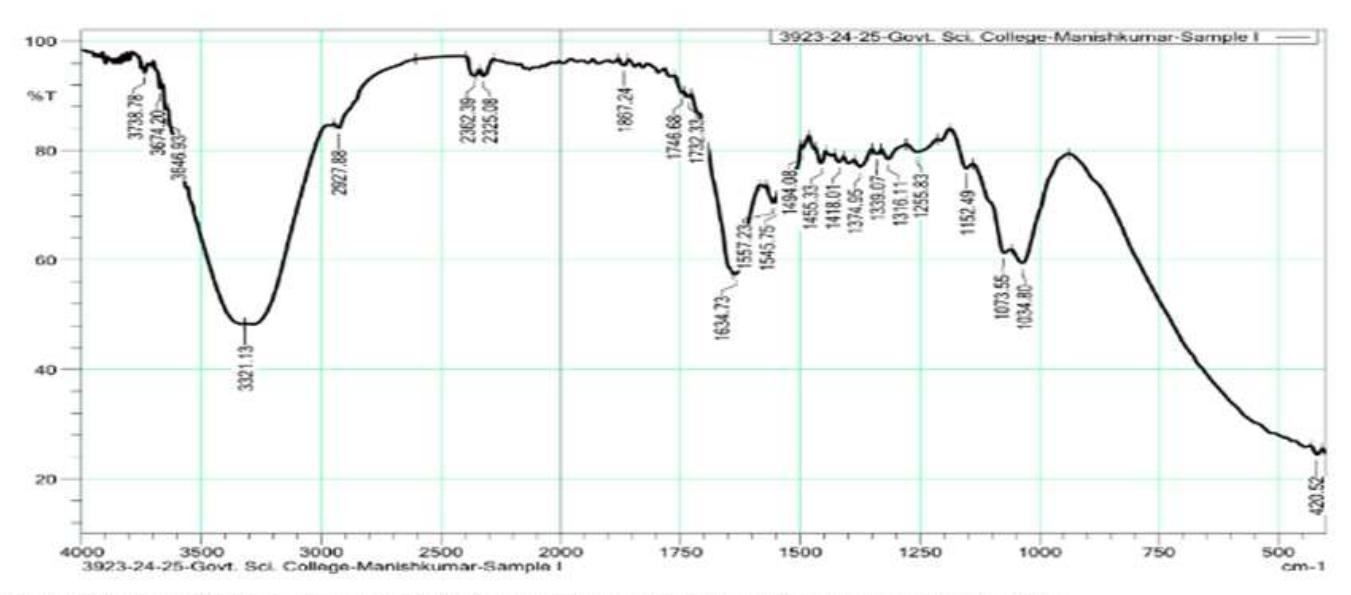


E:\text{E:YDHARAYDATA\text{2025-26\text{August 2025\text{21559-25-26-Govt. Sci. clg-Chemistry dept.-Manish-Plant extract.ispd 1559-25-26-Govt. Sci. clg-Chemistry dept.-Manish-Plant extract

Fig.7a FTIR of Plant Extract

Int. J. Adv. Multidiscip. Res. (2025). 12(11): 17-34

SICART, V.V. Nagar



E:YDHARAYDATAY2024-25¥March 2025¥3923-24-25-Govt. Sci. College-Manishkumar-Sample Lispd

Fig.7b FTIR of AgNPs

Synthesis	Functional Group	Wave number (cm ⁻¹)
Synthesized AgNPs using <i>Chloris virgata</i>	O-H stretching vibration	3646 cm^{-1} .
	typically indicates the presence of O-H or N-H stretching vibrations, often associated with alcohol (O-H) or amine (N-H) functional groups	3321 cm ⁻¹
	indicates the presence of C-H stretching vibrations, specifically from alkanes, alkenes, and carboxylic acids	2827 cm ⁻¹
	Indicates the presence of amide I band or C=O stretching vibrations, often associated with carbonyl groups in proteins, peptides, or amides.	1634 cm ⁻¹
	indicates the presence of C-O stretching vibrations, often associated with alcohols, phenols, and ethers	1073 cm ⁻¹
	indicates the presence of Si-O stretching vibrations or C-N bond vibrations	1034 cm ⁻¹
	indicates the presence of a Silver-oxygen (Ag-O) bond	420 cm ⁻¹

X-Ray Diffraction

X-ray Diffraction (XRD) measurements of the bio-reduced silver nanoparticles was performed using a Bruker Model D8 Advance analytical instrument at 200°C. The sharp diffraction patterns obtained from the XRD spectra indicated that the AgNPs were purely crystalline. Fig. 8 indicates 3 peaks at 20. The measurement profile values of 26.718°, 35.686°, and 57.466° correspond to the (hkl) values of the (1,1,1), (1,1,0), and (1,2,2) planes, respectively, which confirm the presence of a crystalline structure in AgNPs. Here, the AgNP hkl values are (1,1,1), which indicates an octahedral crystal form; (1,1,0), which indicates a rectangular or rhombic

shape; and (1,2,2), which indicates a tetragonal crystal structure and 25.23 nm size on the XRD data and calculation using the Scherrer equation.

$$D=((K\times\lambda))/((\beta\times\cos\theta))$$

Where, D: is the average crystallite size (often in nanometers).

K: is the Scherrer constant, a shape factor that depends on the crystallite shape (typically around 0.8 for spherical or equiaxed crystallites).

 λ : is the wavelength of the X-ray radiation used.

β: is the full width at half maximum (FWHM) of the diffraction peak, after instrumental broadening is accounted for.

 θ : is the Bragg angle of the diffraction peak.

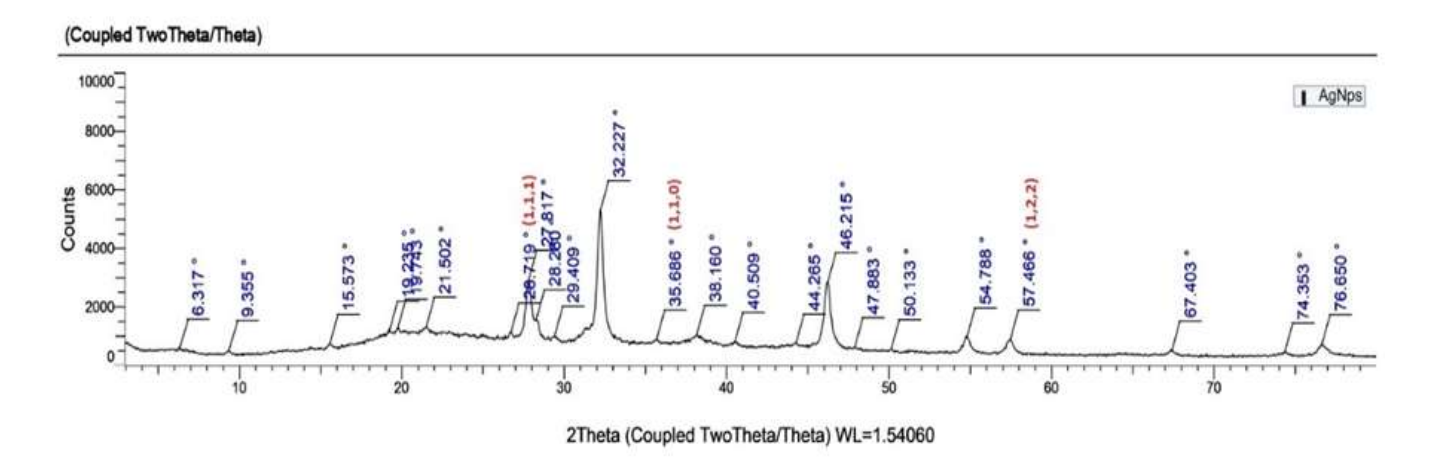


Fig.8 shows XRD of AgNPs

This technique is used to study the structure of materials, particularly crystalline materials. This involves the interaction of X-rays with a sample, resulting in a characteristic diffraction pattern that reveals information about the crystal structure, phase, and other properties of the sample. (R.N. Rai et al.; Karam et al., 2022)

Scanning Electron Microscopy Analysis

Scanning Electron Microscopy Analysis Field Emission Gun- Scanning Electron Microscopic (FEG-SEM) analysis was performed using the JSM-7600F machine and operating at a voltage of 0.1 to 30 kV; for operation, a very small amount of dry powder sample was required to obtain the types of images shown in Figs. 10a, 10b, and 10c. Scanning electron microscopy analysis was carried out to determine the shape and size of the synthesized AgNPs. (Carter et al., 2025; Aigoin et al., 2025) Here, see an image of silver nanoparticles, which are not pores or hollow in nature; they possess a completely solid shape. The obtained NPs were spherical in shape and size, ranging from approximately 8.72 nm, according to the XRD data.

FEG-SEM is a type of scanning electron microscope (SEM) that uses a field emission gun (FEG) as its electron source, enabling a higher

resolution and improved imaging capabilities compared to traditional SEMs.

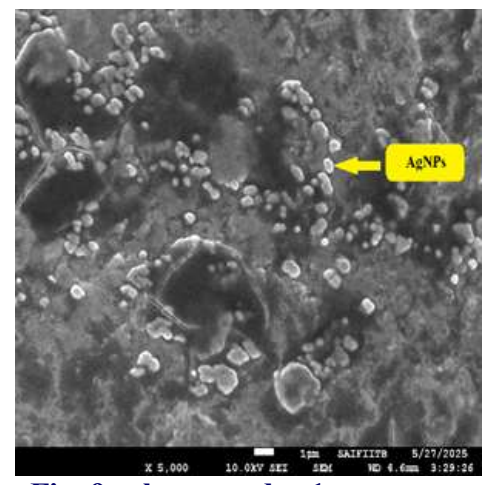


Fig. 9a shows under 1μm range AgNPs with 5K resolution

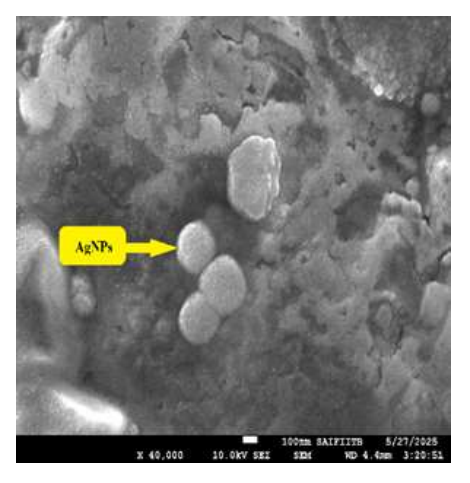


Fig. 9b shows under 100 nm range AgNPs with 40K resolution

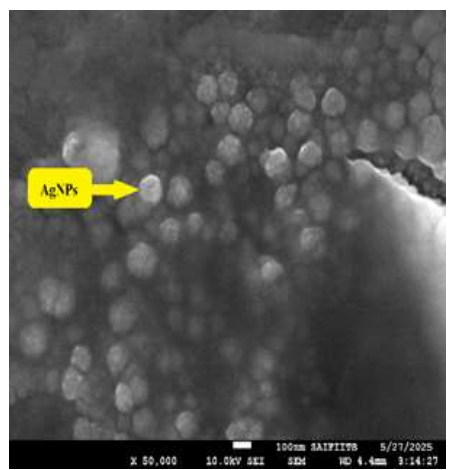


Fig. 9c shows under 100 nm range AgNPs with 50K resolution

High Resolution Transmission Electron Microscopy (HR-TEM) Analysis

This technique uses a focused beam of electrons to create high-resolution images of the internal structure of a material, particularly at the atomic level. (Wang et al., 2015) Here show HR TEM images of silver nanoparticles, which are round in shape, show a completely solid shape in nature.

FEG-TEM at 300 kV (Field Emission Gun Transmission Electron Microscope 300kv) on AgNPs was performed using FEI Tecnai G2 and model number F30. Images of AgNPs synthesized using an aqueous plant extract of *Chloris virgata* shown in Fig.10a, 10b, 10c, 10d, and 10e. The synthesized AgNPs were almost spherical in shape with an average diameter of 5.77 nm minimum value as determined by XRD.

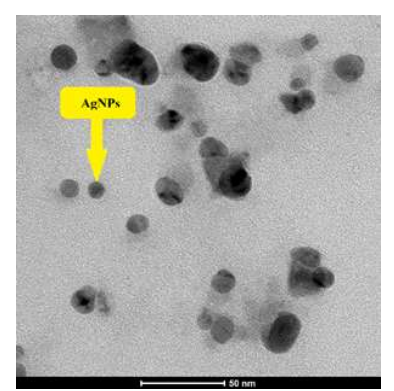


Fig. 10a shows under 50 nm

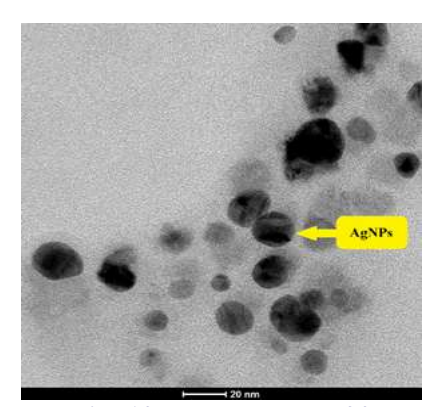


Fig. 10b shows under 20 nm

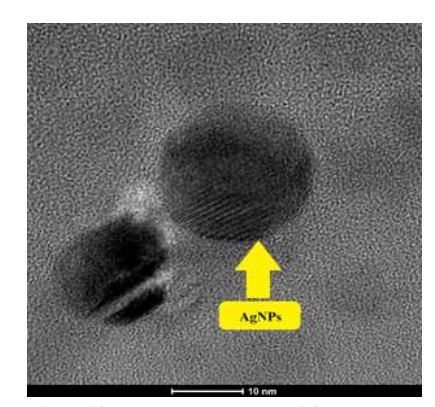
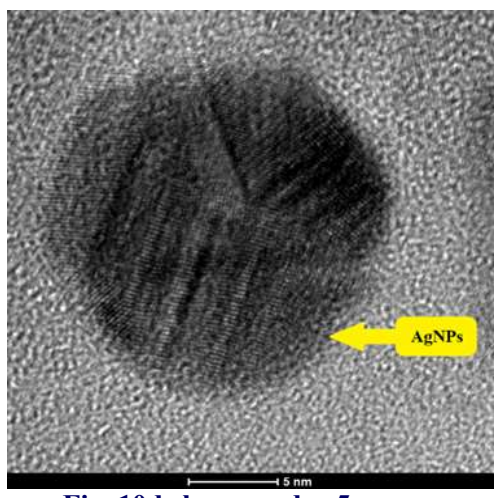


Fig. 10c shows under 10 nm

Int. J. Adv. Multidiscip. Res. (2025). 12(11): 17-34





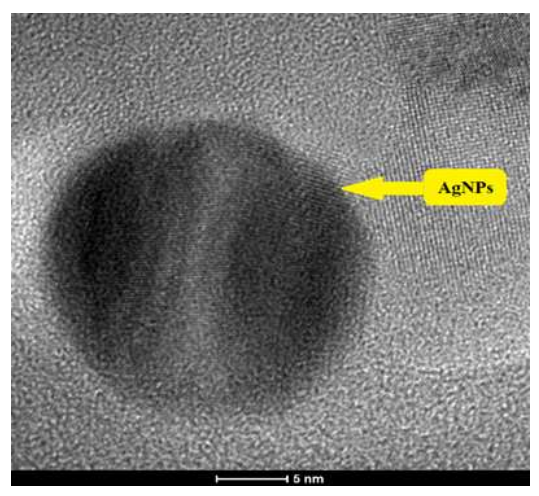


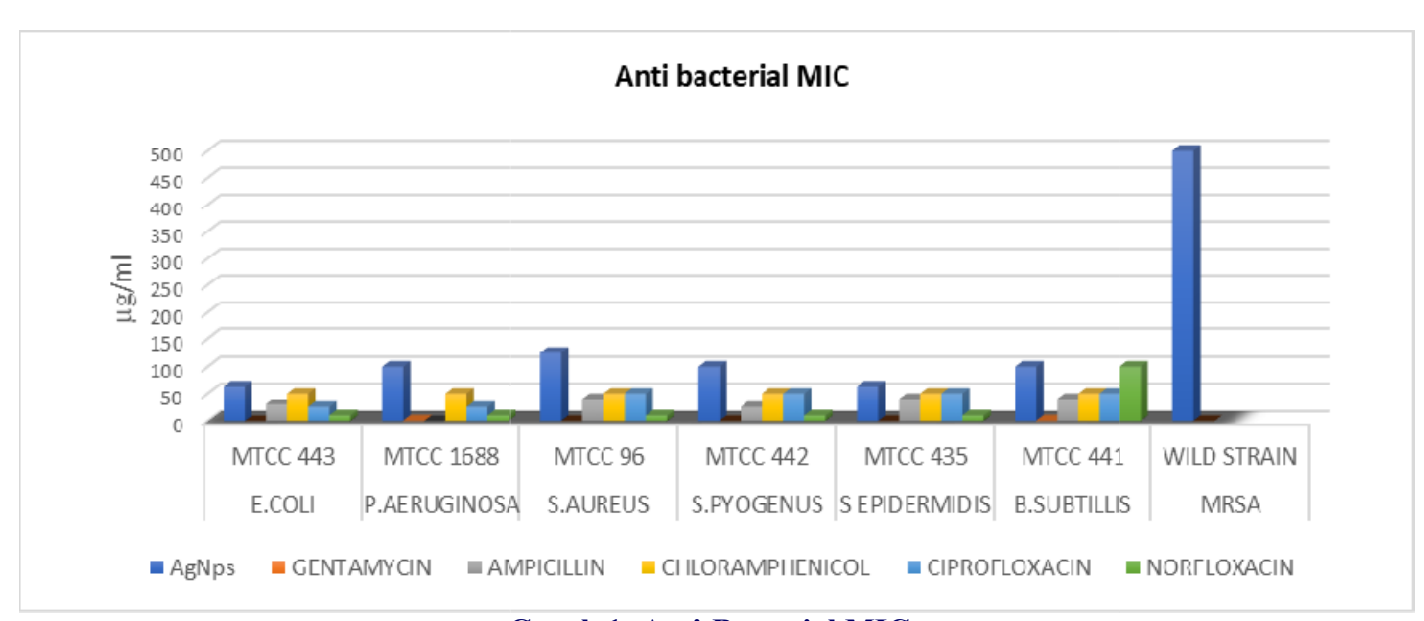
Fig. 10e shows under 5 nm

Biological activities

1. Anti-microbial activity

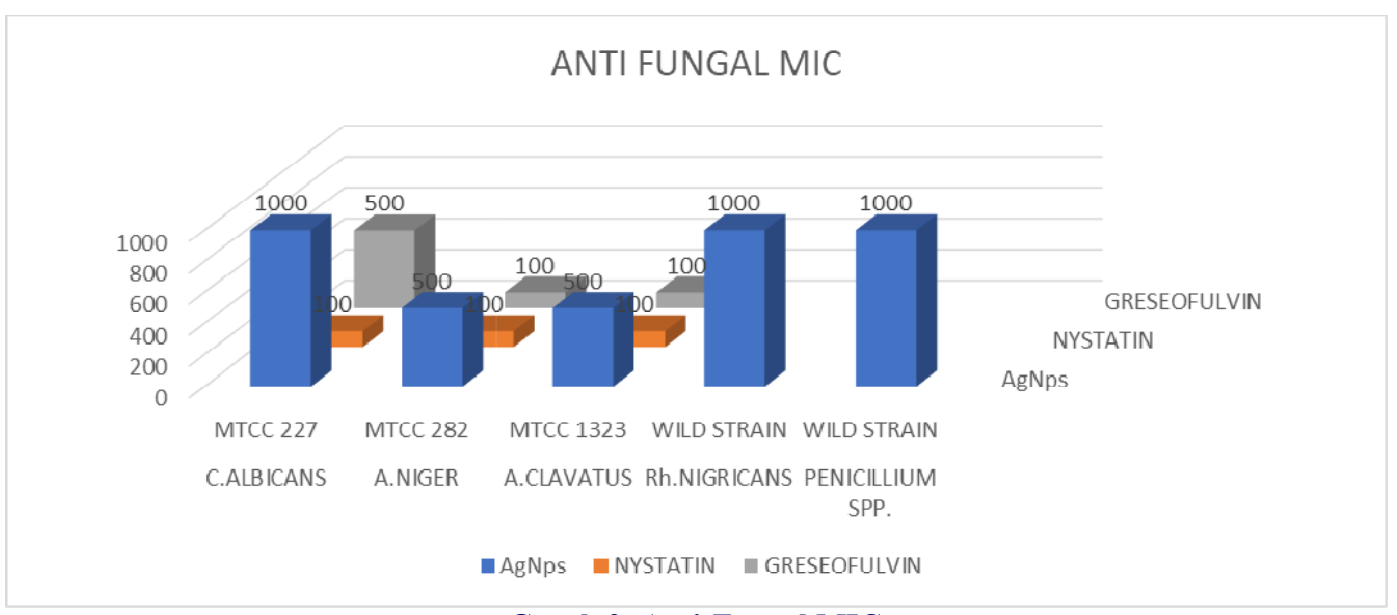
The minimum inhibitory concentration (MIC) was the highest, with at least 88 percent inhibition

zone. The outcome was significantly influenced by the inoculum size. The test mixture contained 10^8 organism/ml.



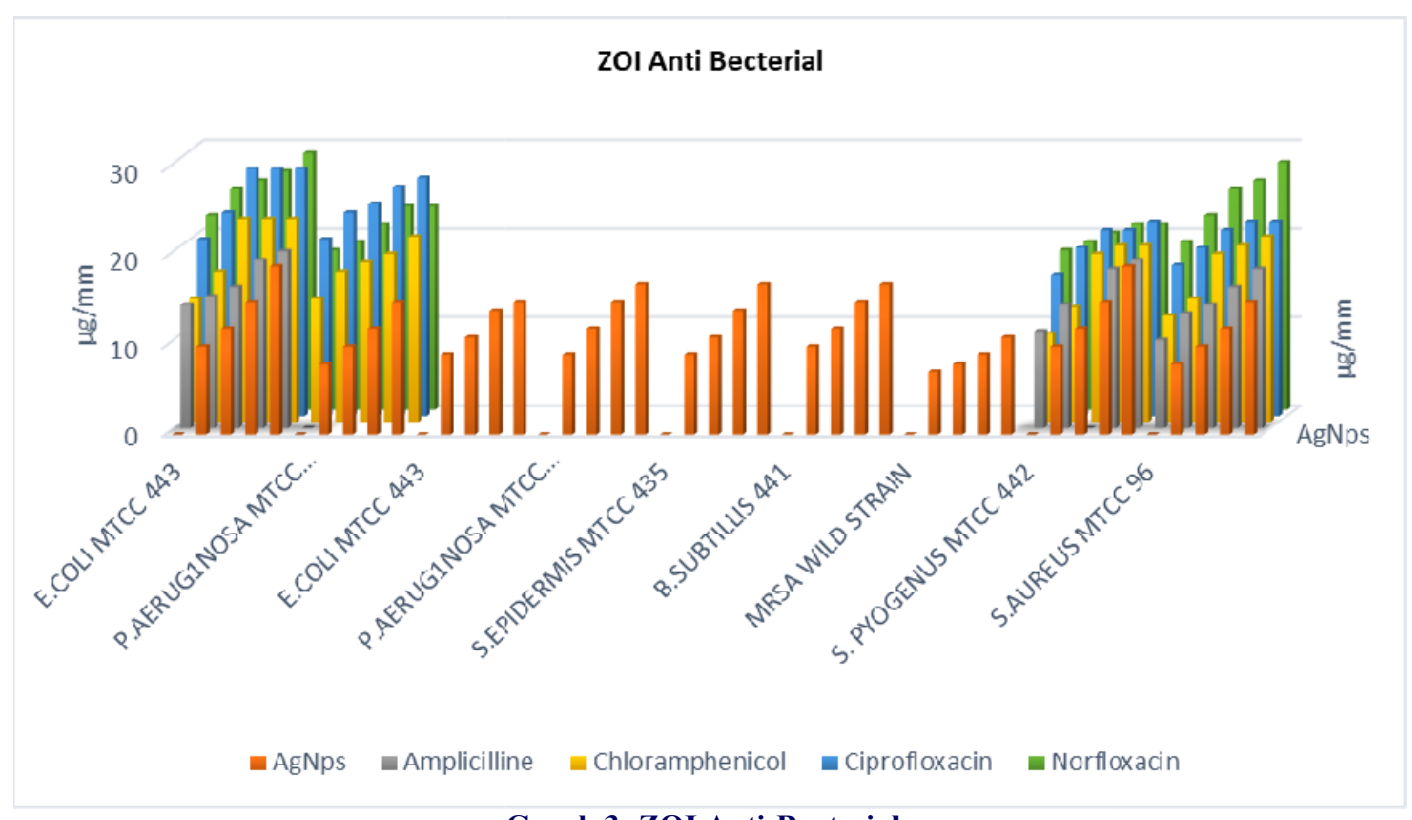
Graph 1: Anti-Bacterial MIC

Int. J. Adv. Multidiscip. Res. (2025). 12(11): 17-34

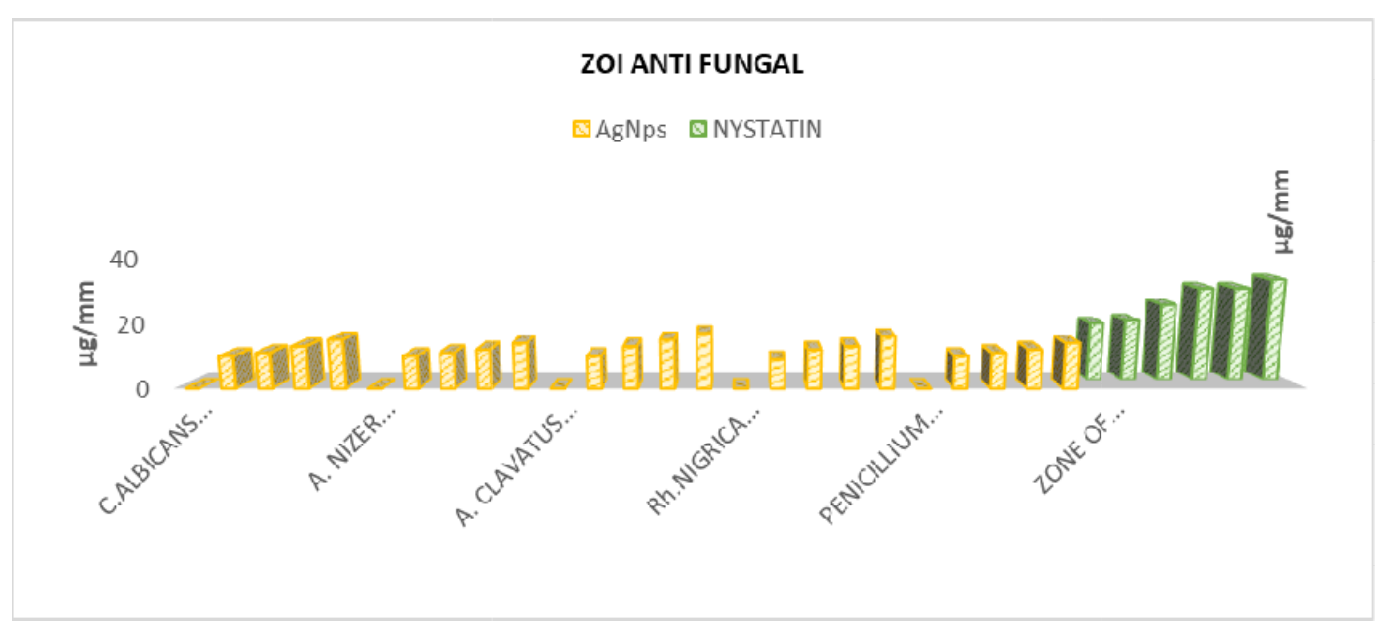


Graph 2: Anti-Fungal MIC

2. Zone of Inhibition (ZOI) for Anti-bacterial and Anti-fungal Activity

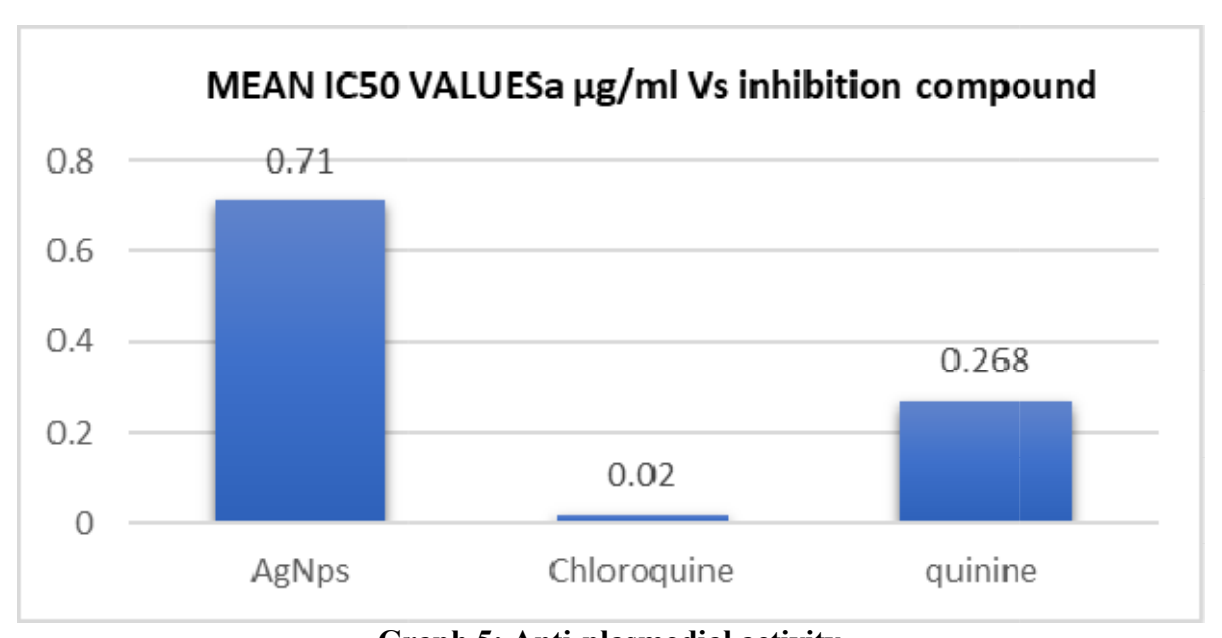


Graph 3: ZOI Anti-Bacterial



Graph 4: ZOI Anti-fungal

3. In Vitro Antimalarial Screening



Graph 5: Anti-plasmodial activity

A safe and easy method for the eco-friendly synthesis of silver nanoparticles using an aqueous plant extract of *Chloris virgata* as a reducing agent under laboratory conditions has been used without the use of poisonous inducers, hazardous chemical additives, and/or elaborate chemical reactions. The formation of AgNPs was detected

visually from a colour change and confirmed using UV-visible spectroscopy (420-465 nm) (Fig.6c) and further authenticated by SEM (Fig. 9a -9c, and XRD (Fig.10). In addition, using FT-IR Spectroscopy, the characteristics of AgNPs were confirmed, as shown in Fig.7b, which showed peaks at 420.52 cm⁻¹ wave numbers

confirming the formation of Ag-O bonds. The particle size was determined c.a. as 25.23 nm. This was further confirmed by TEM studies; moreover, the almost spherical shape of the particles was known using transmission electron microscopy, Fig.10a-10e. The silver nanoparticles exhibited greater anti-bacterial activity and Antifungal activity; Graphs 1 and 2, Graph 3, Graph 4, and Graph 5 sequentially show ZOI Antibacterial, ZOI Anti-fungal, and in vitro antiplasmodial activity.

In this study, biologically active nanomaterials were designed and developed as potent antimicrobial agents using aqueous extracts from Chloris virgata plant, which is an eco-friendly process. The benefit of using this method is that it is less time-consuming, from simple materials obtained from nature to a relatively easy way to synthesize of silver nanoparticles. The Silver Nanoparticles (AgNPs) were characterized by UV-Visible Spectroscopy, FTIR, XRD, SEM, TEM, and their in vitro anti-microbial, ZOI antibacterial, ZOI anti-fungal, and anti-plasmodial investigated. UV-Visible activities were spectroscopy results confirmed the formation of the particles. The change in colour of the solution from dark red to dark brown indicated the reduction of Ag⁺¹ to Ag⁰. FTIR analysis revealed stretching and vibration bands, confirming the presence of various bonds in the sample. The particle size of the silver nanoparticles is 25.20 nm, which was confirmed by XRD and FEG-SEM analyses. Spherical in shape and in the size range of 5.77-52.58 nm of AgNPs were confirmed by HR-TEM analysis, and all were consistent.

Results for Anti-bacterial Activity using Minimum Inhibitory Concentration (MIC) – Graph 1 shows the efficacy of various antimicrobial agents, including silver nanoparticles (AgNPs), against several bacterial strains. AgNPs exhibited higher MIC values (62.5–500 μg/mL), indicating comparatively lower potency than conventional antibiotics. For MRSA (wild-type

strain), AgNPs showed the highest MIC value (500 µg/mL), suggesting reduced effectiveness against resistant strains. Conventional antibiotics like Gentamycin and Norfloxacin showed significantly lower MICs (as low as 0.05–1 µg/mL), indicating higher potency. Despite this, AgNPs still demonstrated anti-microbial activity against all tested bacteria, albeit at higher concentrations. With Zone of Inhibition (ZOI) -Graph 3 results reinforce the MIC findings, AgNPs produced moderate inhibition zones (8–28 reasonable suggesting anti-bacterial activity. The highest ZOI by AgNPs was against S. aureus MTCC 86 (28 mm), whereas the lowest was against MRSA (7 mm). In comparison, standard antibiotics such as Norfloxacin and Ciprofloxacin produced larger ZOIs in many strains, confirming their superior efficacy. Interestingly, AgNPs performed comparably in some strains, such as P. aeruginosa and S. pvogenus, indicating their potential supplementary treatments. For Anti-fungal Activity with Minimum **Inhibitory** Concentration (MIC) - Graph 2 AgNPs exhibited varying Anti-fungal activity across fungal strains. MIC values for AgNPs ranged from 500 to 1000 µg/mL, with C. albicans and wild strains such as Penicillium spp. showing the least susceptibility (1000 µg/mL). Nystatin and Griseofulvin had significantly lower MICs (100-500 µg/mL), confirming their strong Anti-fungal properties. With Zone of Inhibition (ZOI) -Graph 4 data further confirmed the lower Antipotency of AgNPs; AgNPs produced fungal ZOIs between 8 and 17 mm, while nystatin showed higher inhibition zones (up to 32 mm). For A. clavatus and R. nigricans, AgNPs showed promising inhibition, suggesting their potential for targeted applications. However, overall, the activity of AgNPs was inferior to Anti-fungal that of the standard Anti-fungal agents. Results for Anti-Plasmodial Activity show that the antiplasmodial efficacy was evaluated using IC50 values: (Graph 5) AgNPs demonstrated an IC50 of 0.71 µg/mL, which is relatively higher compared to Chloroquine (0.02 µg/mL) and

Quinine (0.268 μ g/mL). This indicates that while AgNPs possess anti-plasmodial activity, their potency is significantly lower than that of established anti-malarial drugs. Nevertheless, the observed activity suggests a potential role in combination therapies or improved drug delivery systems.

Conclusion

AgNPs exhibit broad-spectrum anti-microbial activity, although with reduced efficacy compared to conventional antibiotics, Anti-fungal s, and anti-plasmodial drugs. Their moderate ZOI and MIC values indicate their potential as alternative or adjunctive therapeutic agents, especially in light of their increasing anti-microbial resistance and broad-spectrum efficacy. Further optimization of nanoparticle synthesis and formulation could enhance their bioactivity and clinical relevance. These findings support the growing importance of nanotechnology in anti-microbial research but also emphasize the need for further optimization and targeted delivery.

Acknowledgments

This work is a heartfelt tribute to the author's family, especially to their parents, whose unwavering support and blessings formed the foundation of this achievement. Gratitude is extended to Dr. Kespi Aspi Pithawala for valuable suggestions throughout the research.

Declaration of Funding Acquisition: No funding was received.

References

Abd El Aty, A. Hafr al Batin Phoenix dactylifera L. Leaves Extract as Efficient Catalyst for Green Synthesis of New Silver Nanoparticles with Broad Spectrum Antimicrobial Activity: Characterization and Evaluation Compared to Fungi. Arabian J. Sci. Eng. 2025, xxx, 1–16.

- Ahmad, N.; Malik, M. A.; Wani, A. H.; Bhat, M. Y. Biogenic Silver Nanoparticles from Fungal Sources: Synthesis, Characterization, and Anti-fungal Potential. Microbial Pathogenesis 2024, 183, 106742.
- Aigoin, J., et al. Comparative Analysis of Electron Microscopy Techniques for Hydrogel Microarchitecture Characterization: SEM, Cryo-SEM, ESEM, and TEM. ACS Omega 2025, 10(15), 14687–14688.
- Azam, Z., Ayaz, A., Younas, M., Qureshi, Z., Arshad, B., Zaman, W., Ullah, F., Nasar, M. Q., Bahadur, S., Irfan, M. M., Hussain, S. Microbial Synthesized Cadmium Oxide Nanoparticles Induce Oxidative Stress and Protein Leakage in Bacterial Cells. Microb. Pathog. 2020, 144, 104188.
- Bali, B., Halder, A., Mondal, A. Fluorescence and UV-vis Spectrophotometry: A Dual-Mode Competitive Approach for Selective Sensing of Dopamine. Anal. Methods 2025, 17(25), 5150–5154.
- Barabadi, H., Honary, S., Ebrahimi, P., Alizadeh, A., Naghibi, F., Saravanan, M. Optimization of Myco-Synthesized Silver Nanoparticles by Response Surface Methodology Employing Box-Behnken Design. Inorg. Chem. 2017, 48(2), 33–43.
- Bestgen, В., et al. Safety, Tolerability, Pharmacokinetics. and Antimalarial of MMV533: Activity A Phase 1a First-in-Human, Randomized, Ascending Dose and Food Effect Study, and a Plasmodium Phase 1b falciparum Volunteer Infection Study. Lancet Infect. Dis. 2025, 25(5), 507–518.
- Bhushan, B. Springer Handbook of Nanotechnology, 4th ed.; Springer: [Place unspecified], 2017. DOI: 10.1007/878-3-318-48833-8.
- Bolortuya, B., Kawabata, S., Yamagami, A., Davaapurev, B.-O., Takahashi, F., Inoue, K., et al. Transcriptome Analysis of Chloris virgata, Which Shows the Fastest Germination and Growth in the Major

- Mongolian Grassland Plant. Front. Plant Sci. 2021, 12, 684887. DOI: 10.3389/fpls.2021.684887.
- Carter, J. L. W., et al. A Comparison of Energy Dispersive Spectroscopy in Transmission Scanning Electron Microscopy with Scanning Transmission Electron Microscopy. Ultramicroscopy 2025, 270, 114106.
- CLSI (Clinical and Laboratory Standards Institute). Performance Standards for Antimicrobial Susceptibility Testing, 33rd ed.; CLSI Supplement M100; Clinical and Laboratory Standards Institute: Wayne, PA, 2023.
- CLSI (Clinical and Laboratory Standards Institute). Performance Standards for Antimicrobial Susceptibility Testing; Clinical and Laboratory Standards Institute: Wayne, PA, 2020.
- Cotton Fabrics with Time. Results in Chemistry 2022, 4, 100462.
- De Mel, S., Gruenler, J., Khoury, L., Heynes, A., Fazekas, J., Damaske, K., Galbadage, T., Gunasekera, R. S., Anderson, R. S. Green Synthesis of Silver Nanoparticles Using alba Leaf Extracts Magnolia and Evaluating Their Anti-microbial. Anticancer, Antioxidant, Photocatalytic Properties. Sci. Rep. 2025, 15(1), 23708.
- Do, H. T., Le, T. A. Anti-bacterial Effect of Silver Nanoparticles Prepared Using Pterospermum diversifolium Semi-solid Extract. J. Opt. Photonics Res. 2025, 2(1), 20–26.
- Doan, L., Nguyen, L.T., Nguyen, N.T.N. Modifying Superparamagnetic Iron Oxide Nanoparticles for Doxorubicin Delivery Carriers: A Review. J. Nanopart. Res. 2023, 25, 73.
- Gajbhiye, S., Sakharwade, S. Silver Nanoparticles in Cosmetics. J. Cosmet. Dermatol. Sci. Appl. 2016, 6, 48–53.
- Gangorde, M. C. Green Synthesis of Bio-Active Silver Nanoparticles from Insect Gall

- Extracts as Potent Anti-Microbial Agents. Int. J. Adv. Multidiscip. Res. 2024, 11(7), 8–23.
- DOI: 10.22182/ijamr.2024.11.07.002.
- Gomeceria, M., Miranda, M., Lopez, E. C., Perez, J., Fabrication of Paper-Based Silver Nanoparticle (AgNP) Sensors for Smartphone-Based Colour imetric Detection of Cu (II) in Water. J. Mater. Sci. Forum 2024, 1112, 108–117.
- Hamid, L. L., Ali, A. Y., Ohmayed, M. M., Ramizy, A., Mutter, T. Y. Anti-microbial Activity of Silver Nanoparticles and Cold Plasma in the Treatment of Hospital Wastewater. Kuwait J. Sci. 2024, 51(2), 100212.
- Htwe, Y. Z. N., Abdullah, M. K., Mariatti, M. Water-Based Graphene/AgNPs Hybrid Conductive Inks for Flexible Electronic Applications. J. Mater. Res. Technol. 2022, 16, 58–73. DOI: 10.1016/j.jmrt.2021.11.158.
- Iwuji, C., Saha, H., Ghann, W., Dotson, D.,
 Bhuiya, M. A., Parvez, M. S., Jahangir,
 Z. S., Rahman, M. M., Chowdhury, F. I.,
 Uddin, J. Synthesis and Characterization
 of Silver Nanoparticles and Their
 Promising Anti-microbial Effects. Chem.
 Phys. Impact 2024, 8, 100758.
- Kabeya, J. K., et al. Anti-microbial Capping Agents on Silver Nanoparticles Made via a Green Method Using Natural Products from Banana Plant Waste. Artif. Cells Nanomed. Biotechnol. 2025, 53(1), 28–42.
- Keerthiga, G., Sengottuvel, R., Obli Prakash, P. C., Maghimaa, M. Enhancing Antibacterial and Antibiofilm Activity Using Gymnema sylvestre Mediated Silver Nanoparticles: A Promising Approach in Infection Control. Biomed. Mater. Devices 2025, May 5, 1–6.
- Kojom Foko, L., Pradel, L., et al. Bio-Inspired Synthesis, Characterization, and Biomedical Applications of Optimized Ceiba pentandra Silver Nanoparticles. Biol. Trace Elem. Res. 2025, 1–15.

- Kumar, A., Dixit, C. K., Sahu, S. Nanoparticles: Properties, Applications, and Toxicities. J. Nanoscience Nanotechnol. 2018, 18(7), 3818–3830.
 - DOI: 10.1166/jnn.2018.16302.
- Kumari, D., Chaudhary, P., Yadav, P., Prakash, A., Chaudhary, S., Janmeda, P. Pharmacognostical Analysis, Quantitative Determination, and in vitro Antioxidant Activity of Chloris virgata Sw. Whole Plant. LIANBS 2024, 13(3), 116. DOI: 10.33263/LIANBS133.116.
- Liknaw, T., et al. Aloe vera Leaf Extract as a Sustainable Route for Silver Nanoparticle Synthesis with Enhanced Anti-microbial Activity. Sci. Rep. 2025, 15(1), 22481.
- Maarebia, et al. Synthesis and Characterization of Silver Nanoparticles Using Water Extract of Sarang semut (Myrmecodia pendans) for Blood Glucose Sensors. Indonesia Chimica Acta 2018, 12(1).
- Mahajan, G., Chauhan, B. S. Evaluation of Pre-Emergent Herbicides for Chloris virgata Control in Mung Bean. Plants 2021, 10(8), 1632. DOI: 10.3389/plants10081632.
- Mamand, D. M., et al. Enhanced Optical Properties of Chitosan Polymer Doped with Orange Peel Dye Investigated via UV–Vis and FTIR Analysis. Sci. Rep. 2025, 15(1), 3232.
- Nafa, N., Alhanash, H., Issa, R. Green Synthesis of Silver Nanoparticles and Their Antibacterial Activity Enhancement. Libyan J. Vet. Med. Sci. 2025, 6(1), 7–12.
- Nemčeková, K., Dudoňová, P., Holka, T., Balážová, S., Hornychová, M., Naumowicz, Szebellaiová, V., M., Gemeiner, P., Mackul'ak, T., Gál, M., Svitková, V. Silver Nanoparticles for Biosensing and Drug Delivery: Mechanical Study on DNA Interaction. Biosensors (Basel) 2025, 15(5), 331. DOI: 10.3380/bios15050331. PMID: 40422070; PMCID: PMC12110216.

- Pasieczna-Patkowska, S., Cichy, M., Flieger, J. Application of Fourier Transform Infrared (FTIR) Spectroscopy in Characterization of Green Synthesized Nanoparticles. Molecules 2025, 30(3), 684.
- Plesnicute, R., et al. Eco-Friendly Synthesis of Silver Nanoparticles with Significant Anti-microbial Activity for Sustainable Applications. Sustainability 2025, 17(12), 5321.
- Rajapaksha, P., Orrell-Trigg, R., Shah, D., Cheeseman, S., Vu, K.B., Ngo, S.T., Murdoch, B.J., Choudhury, N.R., Yin, H., Cozzolino, D., et al. Broad Spectrum Anti-bacterial Zinc Oxide-Reduced Graphene Oxide Nanocomposite for Water Depollution. Mater. Today Chem. 2023, 27, 101242.
- Riaz, T., et al. FTIR Analysis of Natural and Synthetic Collagen. Appl. Spectrosc. Rev. 2018, 53(8), 703–746.
- Rieckmann, K. H., Campbell, G. H., Sax, L. J., Mrema, J. E. Drug Sensitivity of Plasmodium falciparum, an in vitro Microtechnique. Lancet 1878, 1, 221–223.
- Rojas-Sandoval, J. Chloris virgata (feather finger grass). CABI Compendium 2022. DOI: 10.1078/cabicompendium.113265.
- S. Sana, S., Dogiparthi, L. K. Green Synthesis of Silver Nanoparticles Using Givotia moluccana Leaf Extract and Evaluation of Their Anti-microbial Activity. Mater. Lett. 2018, 226, 47–51.
- Sahu, S. K., Sahoo, P. R., Dash, S., Mishra, S. R., Behera, P. C. Anti-microbial Activity of Silver Nanoparticles Against Common Bovine Mastitis Pathogens: A Comparative Analysis. Curr. Microbiol. 2025, 82(3), 1–1.
- Saqib, S., Faryad, S., Afridi, M. I., Arshad, B., Younas, M., Naeem, M., Zaman, W., Ullah, F., Nisar, M., Ali, S., Elgorban, A. M. Bimetallic Assembled Silver Nanoparticles Impregnated in Aspergillus fumigatus Extract Damage the Bacterial

- Membrane Surface and Release Cellular Contents. Coatings 2022, 12(10), 1505.
- Saqib, S., Nazeer, A., Ali, M., et al. Catalytic Potential of Endophytes Facilitates Synthesis of Biometallic Zinc Oxide Nanoparticles for Agricultural Application. Biometals 2022, 35, 867–885.
- Sati, A.: Ranade. T. N.; Mali. S. N.; Ahmad Yasin, H. K.; Pratap, A. Silver Nanoparticles (AgNPs): Comprehensive Insights into Bio/Synthesis, Key Influencing Factors. Multifaceted Applications, and Toxicity—A 2024 Update. ACS Omega 2025, 10, 7548-7582. DOI: 10.1021/acsomega.4c11045.
- Simbine, E. O., Rodrigues, L. d. C., Lapa-Guimarães, J. L., Kamimura, E. S., Corassin, C. H., Fernandes de Oliveira, C. A. Application of Silver Nanoparticles in Food Packages: A Review. Food Sci. Technol., Campinas 2018, 38(4), 783–802.
- Singh, R. K., Nallaswamy, D., Rajeshkumar, S., Varghese, S. S. Green Synthesis of Silver Nanoparticles Using Neem and Turmeric Extract and the Anti-microbial Activity of Plant-Mediated Silver Nanoparticles. J. Oral Biol. Craniofac. Res. 2025, 15(2), 385–401.

- Srinivasa, S. B., Ullal, S. N., Kalal, B. S. Quinoline Conjugates for Enhanced Antimalarial Activity: A Review on Synthesis by Molecular Hybridization and Structure-Activity Relationship (SAR) Investigation. Am. J. Transl. Res. 2025, 17(2), 1335.
- Varghese, R. M., Kumar, A., Shanmugam, R. Anti-microbial Activity of Silver Nanoparticles Synthesized Using Ocimum tenuiflorum and Ocimum gratissimum Herbal Formulations. Cureus 2024, 16(2).
- Vu, K. B., Phung, T. K., Tran, T. T. T., Mugemana, C., Giang, H. N., Nhi, T. L. P. Polystyrene Nanoparticles Prepared by Nanoprecipitation: A Recyclable Template for Fabricating Hollow Silica. J. Ind. Eng. Chem. 2021, 87, 307–315.
- Wang, J., et al. Atomic-Scale Strain Field Mapping Methods for HR-TEM and HR-STEM Images. Acta Mech. Solida Sin. 2025, 1–15.
- Yaqoob, A. A., Umar, K., Ibrahim, M. N. M. Silver Nanoparticles: Various Methods of Synthesis, Size Affecting Factors, and Their Potential Applications—A Review. Appl. Nanosci. 2020, 10, 1368–1378.



How to cite this article:

M.C. Gangorde and Vatsal M. Patel. (2025). Phytogenic Silver Nanoparticles: Green Synthesis for their Dual Bioactivity against Microbes and Malaria Parasites. Int. J. Adv. Multidiscip. Res. 12(11): 17-34

DOI: http://dx.doi.org/10.22192/ijamr.2025.12.11.002